DYNAMIC ANALYSIS OF A BEAM RESTING ON AN ELASTIC HALF-SPACE WITH INERTIAL PROPERTIES

S. Guenfoud[a,*], S.V. Bosakov[b], D.F. Laefer[c]

[a]*Mechanics & Structures Laboratory. University of Guelma, Algeria*

[b]*Structural Mechanics department, Belarusian National Technical University, Belarus*

[c]*School of Architecture, Landscape, and Civil Engineering, University College Dublin, Ireland*

Abstract

This work gives a semi-analytical approach for the dynamic analysis of beams and plates resting on an elastic half-space with inertial properties. Such calculations have been associated with significant mathematical challenges, often leading to unrealizable computing processes. Therefore, this paper presents a detailed analysis of Green's function defining surface displacements of such a space in the contact zone with structures, which allows determination of reactive forces and other physical responses. The obtained solutions can be applied to (i) study dynamic interaction between soil and structures, (ii) determine transient wave fields caused by a seismic source, and (iii) assess numerical computations with different numerical methods programs. Natural frequencies, natural shapes, and the dynamic response of a beam due to external harmonic excitation are determined. Eigenfrequencies and Eigenshapes are presented. Validation with a Boussinesq problem illustrates the inertia effect on the results of the dynamic analysis.

Keywords: Green's function; ground inertia; beam; Eigenfrequencies; Eigenshapes; dynamic response.

---

1. Introduction

The analysis of beams and plates resting on an elastic foundation is considered a contact problem, and in both statics and dynamics is a highly topical subject of wide applicability, such as the foundations of buildings and bridges and most underground construction. This problem becomes complicated to solve when the more realistic elements are entered into the calculation, such as complex geometry, material anisotropy, and frictional forces. Foundation inertia, defined as the incorporation of the mass of the medium into the calculation of a structure's dynamic response, is an interesting problem, which strongly influences and complicates calculation. As such, the dynamic analysis of beams and plates in interaction with elastic media has not been to date completely solved, even by using a linear approach to the media's inertia. Improving existing calculation methods of these structures or proposing new methods holds the potential of pioneering safer and cheaper structures, as well as more reliable designs.

Considerable research has been advanced in this domain. The first work in transient wave propagation in elastic solids was established by Lamb [1], later known as Lamb's problem. In this work, wave propagation generated at the surface of an isotropic, homogeneous, elastic half-space by the application of loads at the surface or inside the half-space was considered. This has subsequently been applied in earthquake engineering, geomechanics, foundation engineering, layered elastic half-spaces, general anisotropy, seismology and other complex problems, including several variants of Lamb's problem being of relevance to geodynamics, contact mechanics, elastodynamics, and ultrasonic nondestructive evaluation [2]. Reissner [3] first developed the analytical solution for a vertically loaded cylindrical disk on elastic half-space using Lamb's problem. Later, many investigators (e.g. Shekhter [4] and Bycroft [5]) extended Reissner's solution to study different modes of vibrations within the framework of Lamb's problem. Using Eason's procedure for sur-

face strip impulses, Guan and Novak [7] determined the transient response of an elastic, homogeneous half-space to instantaneously-applied, rectangular loading.

Shinozuka et al. [8] investigated the three-dimensional (3D) wave scattering phenomenon in a layered half-space considering lateral non-homogeneities. Their introduction of lateral non-homogeneities into the earth medium model of a layered half-space resulted in both mathematical and physical complexities. Using the Cagniard–De Hoop method, Jin and Liu [9] obtained the exact solution for the horizontal displacement at the center of the surface of an elastic half-space under horizontal, impulse, punch loading that can be used to study the dynamic interaction between soil and structures using a transient Lamb's solution. An exact solution for the vertical displacement under a vertical, impulse loading with a punch-like distribution and for the horizontal displacement under horizontal, impulse punch loading were developed by Jin [10,11] at the center of the surface of an elastic half-space. While Zhou et al. [12] obtained solutions that can be used to study a variety of transient, wave propagation problems and dynamic interaction between saturated soil and structures. Additionally, Pradhan et al. [13] found impedance functions presented in the form of simple dimensionless graphs, which may prove to be useful in understanding the harmonic response of foundations resting on layered soil under vertical excitation, and Gazetas [14] presented simple formulas for impedance functions, which can be readily used by practicing engineers.

Above is a sampling of the wide applicability and scope of research related to dynamics and elastic half-spaces. In this paper, a detailed study of Green's function (i.e. the displacements of the surface of a half-space with inertial properties due to the vertical load) is presented, and a new approach is created for the dynamic analysis in engineering applications. In addition, these solutions can be applied within the various numerical methods used in more complicated problems.

2. Problem approach

Herein a new approach is proposed to determine the natural frequencies, natural shape, and response to the external load for a beam on an elastic ground with inertial properties based on Lamb's problem [1]. The elastic ground is considered as a homogeneous and isotropic half-space with iner-

tial properties. Moreover, the curvature of the half-space surface, damping, bending movements in the cross direction of the beam and the friction in the contact zone between the beam and the surface of the half-space are neglected. A beam with total mass m and bending rigidity EI resting on the surface of a half-space with inertial properties is considered under external, vertical excitation (Fig. 1).

The proposed approach is based on the method of Zhemochkin and Sinitsyn [15], in which the beam is divided into equal rectangular elements of size c_i (length) and b_i (width). Therefore, continuous contact between the beam and the surface of an elastic half-space is replaced by a discontinuous contact, which ensures a rigid, vertical liaison located in the center of each element (fig. 2). During the vibration, these liaisons become functions of time. To resolve this hyper static system (Fig. 2), the mixed method of structural mechanics as introduced by Zhemochkin and Sinitsyn [15] is employed; details of this method are included Appendix 1. The system's unknowns are the liaison efforts $X_i(t)$, the vertical displacement $u_0(t)$, and angle of rotation $\varphi_0(t)$ of the beam at the embedding point (Fig. 3). The inertia forces $J_i(t)$ vibrating masses are applied only on the beam as reaction efforts $X_i(t)$ are applied on the beam and on the surface of a half-space (Fig. 3).

The canonical equations according to Zhemochkin and Sinitsyn [15] take the form of eq. (1)

$$\begin{cases} \text{M} \\ \sum_{j=1}^{n} (v_{ij} + y_{ij}) X_j(t) - \sum_{j=1}^{n} y_{ij} J_j(t) + \lambda_i \varphi_0(t) + u_0(t) + \Delta_{iP} = 0; \quad i = 1, \text{K}, n \\ \text{M} \\ \sum_{j=1}^{n} [X_j(t) - J_j(t)] \lambda_j = \text{I}_y \ddot{\varphi}_0(t) \\ \sum_{j=1}^{n} [X_j(t) - J_j(t)] = m \ddot{u}_0(t) \end{cases} \tag{1}$$

where v_{ij} is Green's function defining the displacement of the surface of a half-space at the point i due to the unitary force $R_j = 1$ applied at the point j of the same surface and distributed into the

elementary area bc; the term y_{ij} is the deflection of the beam at the point i due to the unitary force $R_j = 1$ applied at the point j of the beam; Δ_{iP} is the function characterizing deflection of the beam at the point i due to external loads; P_p is the external load applied in the point p of the beam (for free vibrations $\Delta_{ip} = 0$); λ_i is the arm of the elementary masse i corresponding to the embedding point; m is the total mass of the beam; and I_y is the inertia moment of the beam corresponding to the axis oy; $\ddot{\varphi}_0(t) = \frac{\partial^2 \varphi_0(t)}{\partial t^2}$; $\ddot{u}_0(t) = \frac{\partial^2 u_0(t)}{\partial t^2}$.

The free vibration of a beam is supposed in the harmonic form, which can be expressed as eq. (2)

$$X_k(t) = X_k e^{i\omega t};\ \varphi_0(t) = \varphi_0 e^{i\omega t}; u_0(t) = u_0 e^{i\omega t}; J_k(t) = J_k e^{i\omega t}, \tag{2}$$

where $X_k; \varphi_0; u_0; J_k$: are amplitude values of $X_k(t)$, $\varphi_0(t)$, $u_0(t)$ and $J_k(t)$ respectively.

Taking into account eq. (2), the system as shown in eq. (1) for free oscillations will take the form of eq. (3)

$$\begin{cases} \mathsf{M} \\ \sum_{j=1}^{n} (v_{ij} + y_{ij}) X_j - \sum_{j=1}^{n} y_{ij} J_j + \lambda_i \varphi_0 + u_0 = 0; \quad i = 1, \mathsf{K}, n \\ \mathsf{M} \\ \sum_{j=1}^{n} [X_j - J_j] \lambda_j = -\omega^2 \mathrm{I}_y \varphi_0 \\ \sum_{j=1}^{n} [X_j - J_j] = -\omega^2 m u_0. \end{cases} \tag{3}$$

3. Green's function for the vertical displacements of the surface of a half-space

Green's function defining the vertical displacements of a half-space surface with inertial properties [1] due to the action of external harmonic load $Pe^{i\omega t}$ is given by eq. (4)

$$v = \frac{-Pe^{i\omega t}}{2\pi G_0}\left[I_\xi + i\pi\chi \mathrm{K} J_0(\chi r)\right]. \tag{4}$$

where P is the harmonic load amplitude; ω the excitation frequency; and r the distance between the point, where the dynamic force is applied and the point where the displacement of elastic half-space surface is determined.

According to Guenfoud et al. [16], after simplifications eq. (4) becomes eq. (5)

$$v = \frac{-kPe^{i\omega t}}{2\pi G_0}\left\{(I_{21} + I_3) + i\left[(I_1 + I_{22}) + \frac{\pi\chi \mathrm{K} J_0(\chi r)}{k}\right]\right\}. \tag{5}$$

where k is the s- wave wavelength $k = \sqrt{\frac{\omega^2\rho}{G_0}}$; ρ is the density of the half-space, $G_0 = \frac{E_0}{2(1+\nu_0)}$, and E_0 and ν_0 elasticity modulus and Poisson's ratio of the half-space, respectively. Considering the external load: $Pe^{i\omega t} = \cos(\omega t)$ and taking into account only the real part of eq. (5), then eq. (6) can be written

$$v = \frac{-k\cos(\omega t)}{2\pi G_0}(I_{21} + I_3). \tag{6}$$

The expressions of I_{21} and I_3 are given in Appendix 2.

For application of the proposed approach, eq. (6) should be integrated over the area of the loaded element with dimensions b and c (fig. 4). Therefore the variable r becomes $r = \sqrt{x^2 + y^2}$, i.e. with

$$v = \frac{-k\cos(\omega t)}{2bc\pi G_0}\int_x\int_y\left[I_{21}\left(\sqrt{x^2 + y^2}\right) + I_3\left(\sqrt{x^2 + y^2}\right)\right]dxdy. \tag{7}$$

Here the expression is divided into the magnitude bc, as loading is considered uniformly distributed across a rectangular element with dimensions b and c. As many authors [e.g. 1, 3, 4] have noted, the basic complexity of this problem lies in the determination of the integral – defined, in this case by eq. (7). Therefore, the problem concerning the determination of the half-space surface dis-

placements must still be solved. In this case as $r \to 0$, the point i coincides with the point j (fig. 4), and thus eq. (7) is integrated over the area of the loaded element assuming a uniformly distributed load. This is shown in eq. (8)

$$v = \frac{-k\cos(\omega t)}{2bc\pi G_0} \int_{-c/2}^{c/2} \int_{-b/2}^{b/2} \left[I_{21}\left(\sqrt{(x-\xi)^2+\eta^2}\right) + I_3\left(\sqrt{(x-\xi)^2+\eta^2}\right)\right] d\eta d\xi \,. \tag{8}$$

Here $r = \sqrt{(x-\xi)^2 + (y-\eta)^2}$ and for the presented case $y = 0$, (fig. 4). Some parts of the integrals I_{21} and I_3 in formulas (8) are calculated without difficulty, but other parts are not evaluated, because of their complexity. Therefore, to resolve this problem Johnson's approach [17] is applied, in which a change of variables from a Cartesian coordinate system into a polar coordinate system is executed, thereby allowing the determination of the displacement of a diagonally offset point (fig. 4). After introducing Johnson's approach, eq. (8) becomes eq. (9):

$$\begin{aligned} v = \frac{-2k\cos(\omega t)}{bc\pi G_0} \Bigg\{ & \int_0^{\arctan\left(\frac{b}{c}\right)} \int_0^{\frac{c}{2\cos\varphi}} \left[I_{21}\left(\sqrt{(x-\xi)^2+\eta^2}\right) + I_3\left(\sqrt{(x-\xi)^2+\eta^2}\right)\right] r dr d\varphi + \\ & + \int_0^{\arctan\left(\frac{c}{b}\right)} \int_0^{\frac{b}{2\cos\theta}} \left[I_{21}\left(\sqrt{(x-\xi)^2+\eta^2}\right) + I_3\left(\sqrt{(x-\xi)^2+\eta^2}\right)\right] \Bigg\} r dr d\theta \end{aligned} \tag{9}$$

This allows consideration of singularity, which is observed as terms $\frac{1}{\sqrt{k^2 r^2}}$ and $Y_0(\chi kr)$ in the expression of I_3, as further described in Appendix 2. In this case, $r \neq 0$ (i.e. the total absence of singularity in all terms of I_{21} and I_3), and the displacements of the surface of a half-space with inertial properties expressed by eq. (6) are calculated with eq. (7). For example, if the loaded element is divided into 16 smaller (fig. 5) elements, then the expression of the displacements of the half-space surface with inertial properties takes the form of eq. (10).

$$v = \frac{-k\cos(\omega t)}{2\pi G_0} \left\{ \frac{1}{16} \sum_{n=1}^{16} \left[I_{21}\left(\sqrt{(x-\xi_n)^2+\eta_n^2}\right) + I_3\left(\sqrt{(x-\xi_n)^2+\eta_n^2}\right)\right]\right\}. \tag{10}$$

Equation 10 defines the displacements of the half-space surface with inertial properties, but gives a long and cumbersome expression. Furthermore, eq.s (9) and (10) must be applied with care since for large values of kr certain instabilities arise, apparently caused by the hypergeometric functions ${}_pF_q(a;b;kr)$, as shown in Fig. 6.

To avoid this instability, I_{21} and I_3 must be decomposed in series and then the angular point's method introduced by Johnson [17] be applied. When the decompositions of I_{21} and I_3 in series of degree 10, the expressions in eq. (11) arise.

$$\begin{aligned} I_{21}+I_3 \cong & -0.6387/kr+0.13+0.14\ln(1.07236k)+0.14\ln(r)+0.15287kr \\ & +\left[0.15k^2-0.04k^2\ln(1.07236k)-0.04k^2\ln(r)\right]r^2-0.019k^3r^3 \\ & +\left[-0.00044k^4+0.0029k^4\ln(1.07236k)+0.0029k^4\ln(r)\right]r^4+0.000898k^5r^5 \\ & +\left[0.00012k^6-0.000094k^6\ln(1.07236k)-0.000094k^6\ln(r)\right]r^6-0.000021k^7r^7 \\ & +\left[-3.035\times10^{-6}k^8+1.69\times10^{-6}k^8\ln(1.07236k)+1.69\times10^{-6}k^8\ln(r)\right]r^8+2.99\times10^{-7}k^9r^9 \\ & +\left[4.14\times10^{-8}k^{10}-1.94\times10^{-8}k^{10}\ln(1.07236k)-1.94\times10^{-8}k^{10}\ln(r)\right]r^{10} \end{aligned} \tag{11}$$

Unfortunately, the problem remains unsolved since as the instability for large values of kr persists. Subsequently, other variants of resolution using the angular point's method were applied.

According to Guenfoud et al. [16], the displacements of the half-space surface with inertial properties due to the action of a uniformly distributed load on a rectangle element with dimensions $c\times b$ (Fig. 5) can be expressed by eq. (12) with expressions of $\Phi_2(\theta)$ and $\Phi_4(\theta)$, as defined in Appendix 3.

$$v=\frac{-k}{2\pi G_0}\cos(\omega t)\int_0^b dy\int_0^a dx\left[\int_{1/2}^{1}\Phi_2(\theta)J_0\left(k\theta\sqrt{x^2+y^2}\right)d\theta+\int_1^{\infty}\Phi_4(\theta)J_0\left(k\theta\sqrt{x^2+y^2}\right)d\theta\right]. \tag{12}$$

Representation of such approximations for $\Phi_2(\theta)$ and $\Phi_4(\theta)$ allows evaluation of eq. (12):

$$\Phi_2(\theta)=\sum_{l=1}^{11}b_{2l-1}\theta^{2l-1};\qquad \Phi_4(\theta)=d_0+\frac{d_1}{\chi-\theta}+\frac{d_2}{\theta^3}. \tag{13}$$

where, d_0, d_1, d_2, b_1, b_3,…, b_{21} coefficients are determined by the least square method, Demidovich et al. [18]. Afterwards, the first integral in the eq. (12) after integration of θ can be represented in the form of eq. 14.

$$\int_0^b dy \int_0^a dx \int_{1/2}^1 \sum_{l=1}^{11} b_{2l-1} \theta^{2l-1} J_0\left(k\theta\sqrt{x^2+y^2}\right) d\theta = \sum_{l=1}^{11} b_{2l-1} F\left(\frac{1}{2},1,2l-1,a,b\right). \tag{14}$$

where $F\left(\frac{1}{2},1,2l-1,a,b\right)$ is defined by the expressions in eq. 15

$$\begin{aligned}
&F(\alpha,\beta,l,a,b) = 4\sum_{m=0}^{\infty}\sum_{n=0}^{\infty}\left(\frac{b}{a}\right)^{2n+1}\sum_{R=0}^{\infty}(2m+2n+2R+2)J_{2m+2n+2R+2}(ka)\times \\
&\times\sum_{s=0}^{\infty}\frac{(-1)^s\Gamma(2m+2n+R+s+2)}{s!(R-s)!\Gamma(2m+s+2)}{}_2F_1\left(-s,-2m-s-1;2n+2;\frac{b^2}{a^2}\right)\times \\
&\times\left[\frac{\beta^{2m+2n+2s+l+1}-\alpha^{2m+2n+2s+l+1}}{\Gamma(2n+2)(2m+2n+2s+l+1)}\right]+8\sum_{i=1}^{\infty}(-1)^i\sum_{m=1}^{\infty}\sum_{n=1}^{\infty}\left(\frac{a}{b}\right)^{2i+2n+1}\sum_{R=0}^{\infty}(4i+2m+2n+2R+2)\times \\
&\times J_{4i+2m+2n+2R+2}(ka)\sum_{s=0}^{\infty}\frac{(-1)^s\Gamma(4i+2m+2n+R+s+2)}{s!(R-s)!\Gamma(s+2i+2m+2)}\times \\
&\times\left[\frac{\beta^{4i+2m+2n+2s+l+1}-\alpha^{4i+2m+2n+2s+l+1}}{(2m+2n+2i+2s+l+1)}\right]{}_2F_1\left(-s,-s-2i-2m-1;2i+2n+2;\frac{b^2}{a^2}\right).
\end{aligned} \tag{15}$$

Equation (15) is resolved using the representation of Baily for the product of two of Bessel's functions as expressed by Bateman and Erdelyi [19]. For the second integral in the eq. (12), there are the following forms based on eq. (15)

$$d_0\int_1^{\infty}\int_0^a\int_0^b J_0(k\theta\sqrt{x^2+y^2})\,dy\,dx\,d\theta = \frac{d_0}{k}\left(a\,arcsh\left(\frac{b}{a}\right)+b\ln\frac{\sqrt{a^2+b^2}}{b}\right)-\frac{d_0}{k^2}F(0,1,1,0,a,b);$$

$$\begin{aligned}
d_1\int_1^{\infty}\int_0^a\int_0^b\frac{J_0(k\theta\sqrt{x^2+y^2})}{\chi-\theta}\,dy\,dx\,d\theta &= \frac{d_1}{\chi}\int_1^{\infty}\int_0^a\int_0^b\sum_{m=1}^{\infty}\frac{\theta^m}{\chi^m}J_0(k\theta\sqrt{x^2+y^2})\,dy\,dx\,d\theta \\
&= -\frac{d_1}{k^2}\sum_{m=1}^{\infty}\frac{1}{\chi^{m+1}}F(0,1,m,a,b),
\end{aligned}$$

$$d_2\int_1^{\infty}\int_0^a\int_0^b\theta^{-3}J_0(k\theta\sqrt{x^2+y^2})\,dy\,dx\,d\theta = d_2\times F(1,\infty,-3,a,b)$$

Despite these significant efforts, the instability was not fully eliminated. After a number of numerical experiments, it was determined that the values of the hypergeometric functions argument must be introduced in the form of a natural fraction number and not in the form of a decimal number. By applying this modified approach, the instability vanishes as described in detail below.

4. Example

Using the following hypergeometric function: $f(z)={}_1F_2\left(9;1,10;\frac{-z^2}{4}\right)$, according to its graphic, certain instability is observed corresponding to the change of its argument z in the interval $[35;41]$. However if the value of its argument z is introduced in the form of natural fraction number, then this instability vanishes (fig. 7). Since the displacements of the surface of a half-space are considered equal to the beam deflection (i.e. $y_k \equiv v_k$) the inertia force J_k can be given by eq. (16)

$$J_i = -M_i \frac{d^2 y_i(t)}{dt^2} = -M_i \frac{d^2 v_i(t)}{dt^2} = M_i \omega^2 \cos(\omega t) v_i . \tag{16}$$

where $v_i = \frac{-k}{2\pi G_0} \sum_{j=1}^{n} X_j F_{ij}$, here $F_{ij} = I_{21} + I_3$.

Taking into account the preceding formulas defining the system parameters (3), the system can now be represented in the following matrix form of eq.s (17) and (18):

$$[A]\begin{bmatrix} X_1 \\ \mathsf{M} \\ X_n \\ \varphi_0 \\ u_0 \end{bmatrix} = \begin{bmatrix} 0 \\ \mathsf{M} \\ \mathsf{M} \\ \mathsf{M} \\ 0 \end{bmatrix}, \tag{17}$$

$$[A] = \begin{bmatrix} A_{11} & \mathsf{L} & A_{1n} & \lambda_1 & 1 \\ \mathsf{M} & \mathsf{O} & \mathsf{M} & \mathsf{M} & \mathsf{M} \\ A_{n1} & \mathsf{L} & A_{nn} & \lambda_n & 1 \\ A_{n+1,1} & \mathsf{L} & A_{n+1,n} & \mathrm{I}_y \omega^2 & 0 \\ A_{n+2,1} & \mathsf{L} & A_{n+2,n} & 0 & m\omega^2 \end{bmatrix}. \tag{18}$$

where A_{ij} are the matrix terms resulting from the mathematic transformation after the introduction of the preceding expressions of all parameters into the system (3). Thus, it is possible to show that the matrix is symmetric according to its main diagonal taking into account eq. (19)

$$\sum_{i=1}^{n} J_i \lambda_i = \omega^2 \mathrm{I}_y \varphi_0; \ \sum_{i=1}^{n} J_i = \omega^2 m u_0. \tag{19}$$

When considering the case of a beam with rigidity EI resting on the surface of a half-space with inertial properties, the above relationships can be applied. Dividing the beam into 10 elements of length $c = \mathrm{l}/5$ and considering that the point of embedment coincides with the centre of mass (fig. 8), values for the deflections y_{ik} of the beam due to the unit force can be determined by the multiplication of the moment diagrams. The deflections values of this type of discretization are shown in the appendix. Values of v_{ik} were determined by the eq. (9) and (10).

The determination of the beam's Eigenfrequencies is done by resolving the equation of the determinant of the system matrix (18). Within this long and complicated equation, the roots represent the Eigenfrequencies values of the beam. Taking $\mathrm{M}_1 = \mathrm{M}_2 = \mathrm{L} = \mathrm{M}_{10} = m/10$, it is found that $\mathrm{I}_y = \frac{250}{3}\mathrm{M}c^2$. The calculation of the roots of the equation is executed numerically using "Mathematica". Figure 9 represents the equation's graph of the determinant, for which the first seven roots representing the first seven values of the beam's Eigenfrequencies are clearly seen. The spectrum of Eigenfrequencies (in Hz) takes into account the geometrical and mechanical properties of the half-space, and the beam involves the following:

$b = 1\,m; \mathrm{M}_i = 1250\,kg\,; E = 2.1 \times 10^{10}\,N/m^2; h = 0.5\,m;$

$2\mathrm{l} = 10m; G_0 = 1.125 \times 10^7\,N/m^2; \nu_0 = 1/3; \rho = 2000\,kg/m^3.$

$\omega_1 = 57.5535,\ \omega_2 = 112.7495,\ \omega_3 = 229.3025,\ \omega_4 = 280.8825,\ \omega_5 = 291.5572,$

$\omega_6 = 303.93538, \ldots$

Determination of the natural shapes of a beam resting on the surface of a half-space with inertial properties requires determination of the natural shape corresponding to each Eigenfrequency. To achieve this value of the unit, the unknown X_1 in the system is defined (19), the first equation is excluded, and the system is solved with $n+1$ equations and $n+1$ unknowns. Subsequently, the natural shapes of the beam are determined by the formula introduced by Zhemochkin and Sinitsyn [15]:

$v_i = \frac{-k}{2\pi G_0} \sum_{j=1}^{n} X_j F_{ij}$, for given discretization: $i = 1,\mathsf{K}\ ,n$; $n = 10$.

The application of these operations allows the determination of the beam's natural shapes for the first six forms

5. Comparison of results

Eigenfrequencies and natural shapes are necessary for the dynamic analysis of any structure. Therefore, much about this problem has been widely reported in the literature, but no relevant case was found concerning the natural frequencies and natural shapes of a beam resting on the surface of a half-space with inertial properties (Lamb's problem). Therefore the comparison was made with the same beam resting on the surface of an elastic half-space with distributive properties (Boussinesq's problem). The difference between the two models (half-space with inertial properties and half-space with distributive properties) according to the proposed approach is presented in the parameter v_i defining the half-space surface displacements. For the half-space with distributive properties, v_i is determined by the following formula:

$v_i = \frac{1-\nu_0^2}{bc\pi E_0} F_{ij}$, where $F_{ij} = \int_{-c/2}^{c/2} \int_{-b/2}^{b/2} \frac{d\eta d\xi}{\sqrt{(x-\xi)^2 + \eta^2}}$.

The same application allows the determination of the natural shapes of the beam resting on this type of foundation. For such a model, the first six forms were obtained as shown in fig. 10 and fig. 11, where the first form is similar but the others differ. This distinction is also observed in the val-

ues of the Eigenfrequencies. This is explained by the influence of the half-space inertia on the dynamic analysis.

6. Response of a beam resting on the surface of a half-space with inertial properties due to the external, vertical excitations

A related issue is the forced vibrations of the beam. This problem concerns the reaction of the beam resting on the surface of a half-space, with inertial properties due to dynamic, external vertical loads. The case presented is of the action of a beam at point 5 (fig. 8) caused by the vertical harmonic load, where the external, vertical harmonic load is varied according to eq. (20):

$$P_p = P_5 = P_0 \cos(2 \times \pi \times f \times t), \tag{20}$$

where P_0 is the amplitude of excitation; f is the frequency of excitation; t is the time of excitation and the values $P_0 = 112500\,N$ and $f = 150\,Hz$ are employed. Obtaining the response requires the resolution of the system (1). In this case, the parameter Δ_{ip} is determined by eq. (21) introduced by Zhemochkin and Sinitsyn [15]:

$$\Delta_{ip} = \sum_{p=1}^{n} y_{ip} P_p = y_{i5} P_5 . \tag{21}$$

where y_{ip} is the beam deflections at the point i due to the external load P_p applied on a beam at a point p. These deflections are determined by the multiplication of the moment diagrams due to the external loads P_p. The solution of the system (1) for the forced oscillations gives the unknowns X_i values varying with the time of excitation. Unknowns X_i represent reactive efforts in the contact zone. In this case, the value's variability is expressed by eq. (22):

$$X_i(t) = X_i(t_0)\cos(2 \times \pi \times f \times t), (i = 1,\mathrm{K}\ ,10) . \tag{22}$$

Finally, the beam displacements during the time of excitation t, representing its response, are determined by eq. (23):

$$v_i = \frac{-k}{2bc\pi G_0} \sum_{j=1}^{10} X(t) F_{ij} \,. \tag{23}$$

Figure 12 shows the vertical displacements variability v_i of the entirety of the beam resting on the surface of a half-space with inertial properties due to the dynamic external load P_5 at each moment $t_j = t_0 + \Delta t$. Here, $t_0 = 0\,s; \Delta t = 0.001\,s$. Furthermore, the maximum displacement is obtained at the point at which the external excitation is applied; note the sign changes in the beam end displacement due to (i) its considerable length and (ii) the near central load application.

Figure 13 shows the vertical displacement variability of the beam v_5 at the point where the dynamic load P_5 is applied, depending upon frequency variation. According to this diagram, the beam's displacement $v_5 \to \infty$, when the frequency value approaches Eigenfrequencies (i.e. appearance of the resonance), since the beam is studied by neglecting damping. In contrast, fig. 14 compares the vertical displacement variability of the beam v_5 at the point where the dynamic load is applied, where (I) is the foundation with inertial properties' model and (II) the foundation with a distributive properties' model. Of note is that the vertical displacements of the beam for the half-space with inertial properties are always less than the same type of displacements, when the inertia of half-space is neglected, thus proving that the half-space inertia fundamentally influences the dynamic analysis. Additionally, the proposed model can account for various dynamic loading type (vertical harmonic, horizontal harmonic, impulse, earthquake and mobile), as well as ondulatory displacements phenomena. The example present in this paper concerns a simple case of loading only to show the efficiency of the approach. The inertia of media (Lamb's model) is an important factor, which other methods neglect and its impact is seen in the beam's response when compared with a Boussinesq based solution.. Furthermore the proposed model can also account for radiation damping, but the approach given in this paper does not consider it as the damping phenomena is neglected.

7. Conclusion

Using a semi-analytic approach, a dynamic analysis of beams resting on the surface of an elastic half-space with both distributive properties and inertial properties was conducted to determine the Eigenfrequencies, the natural shapes, the beam response to external dynamic loads, and the internal forces in the beam sections. Determination of the reactive forces in the contact zone representing the interaction phenomena between beam and half-space surface is necessary to find others physical magnitudes. For this purpose, it is imperative to study Green's function defining the displacements of the contact zone (i.e. contact problem phenomena). This function represents substantial challenges, when the inertia of an elastic half-space is considered (Lamb's problem). The proposed relationships successfully overcome the instability problem caused by the hypergeometric functions, which has represented a great challenge to the study of the ondulatory phenomenon of the displacements associated with this problem. Additionally, the obtained solution is semi-analytical and can, therefore, be readily computed to be more compatible with engineering applications than previous approaches and can effectively be used as an approximation function in different numerical methods to handle more complicated problems of wave propagation in dynamics. As such, this work represents a fundamental advance in the solving of more complicated dynamics problems. As verification, the calculated results compared satisfactorily to the same beam resting on the surface of an elastic half-space with distributive properties (Boussinesq's problem).

References

[1] Lamb H. On the propagation of tremors over the surface of an elastic solid. Philos Trans R Soc London 1904;A203: p.1–42.

[2] Graf K.F. Wave motion in elastic solids. Courier Dover Publications; 1991.

[3] Reissner E. Stationare, axialsymmetrische, druch ein schuttelnde Masse erregte Schwingungen eines homogenen elastische Halbraumes. Ingenieur Archiv 1936;7(6):381–396.

[4] Shekhter O.Y. The taking into account of the inertial properties of the ground in the calculation of a foundation unit on forced vibration. The work's collection of N.I.I.O., vibration of constructions and foundations 1948;(2):p.72–89; (Russian Edition).

[5] Bycroft G.N. Forced vibrations of a rigid circular plate on a semi infinite elastic space and on an elastic stratum. Philos Trans R Soc Lond 1956;248(A.948):327–68.

[7] Guan F., Novak M. Transient response of an elastic homogeneous halfspace to suddenly applied rectangular loading. Journal of Applied Mechanics: ASME 1994;61:256–263.

[8] Shinozuka M., Deodatis G., Zhang R., Papageorgiou A.S. Modeling, synthetics and engineering applications of strong earthquake wave motion. Soil Dynamics and Earthquake Engineering 1999;18:209–228.

[9] Jin B., Liu H. Exact solution for horizontal displacement at center of the surface of an elastic half-space under horizontal impulsive punch loading. Soil Dynamics and Earthquake Engineering 1999;18(7): p.495–498.

[10] Jin B. Elastic halfspace under impulsive, distributed, vertical loading at surface: exact solution at center for a punch-like distribution. Soil Dynamics and Earthquake Engineering 1998;17(5):311–316.

[11] Jin B. Exact solution for horizontal displacement at center of the surface of an elastic half-space under horizontal impulsive punch loading. Soil Dynamics and Earthquake Engineering 1999;18:495–508.

[12] Zhou X.L., Wang J.H., Lu J.F. Transient foundation solution of saturated soil to impulsive concentrated loading. Soil Dynamics and Earthquake Engineering 2002;22:273–281.

[13] Pradhan P.K., Baidya D.K., Ghosh D.P. Dynamic response of foundations resting on layered soil by cone model. Soil Dynamics and Earthquake Engineering 2004;24:425–434.

[14] Gazetas G. Formulas and charts for impedances of surface and embedded foundations. J Geotech Engng ASCE1991;117(9):1363–81.

[15] Zhemochkin B.N., Sinitsyn A.P. Practical methods of the calculation of beams and plates resting on an elastic foundation. Moscow: Stroyizdat publishing company 1962; (Russian Edition).

[16] Guenfoud S., Amrane M.N, Bosakov S.V., Ouelaa N. Semi-analytical evaluation of integral forms associated with Lamb's problem. Soil Dynamics and Earthquake Engineering (2008), doi:10.1016/j. soildyn.2008.04.007.

[17] Johnson K. Contact interaction's mechanics. Moscow: Mir publishing company 1989; (Russian Edition).

[18] Demidovich B.P., Maron I.A., Shuvalov E.Z. Numerical analysis methods. Moscow: Nayka publishing company 1967; (Russian Edition).

[19] Bateman H., Erdelyi A. Higher transcendental functions, Volume 2. Moscow: Mir publishing company 1983; (Russian Edition).

[20] Gradshteyn I.S., Ryzhik M.I. Tables of integrals, series and derivations. Moscow: FM publishing company 1969; (Russian Edition).

FIGURE CAPTIONS

Fig. 1. Beam resting on the surface of an elastic half-space with inertial properties subjected to external, vertical excitation

Fig. 2. Beam divided into elements to ensure a rigid, vertical liaison located in the center of each element

Fig. 3. Discretization of the system beam and half-space showing the forces and unknowns of the hyper static system

Fig. 4. Geometry of the loaded element showing the area over which the integration should occur

Fig. 5. The loaded element is divided into smaller elements allowing expression of the displacements of the half-space surface with inertial properties to take the form of eq. 10.

Fig. 6. Variability of the function ${}_pF_q(a;b;kr)$ still vulnerable to instability at large values of kr

Fig. 7. Graphic representation of the correction of the instability of function ${}_1F_2(9;1,10;-z^2/4)$

Fig. 8. Beam on the surface of an elastic half-space with inertial properties divided into 10 elements allowing deflection determination by multiplication of the moment diagrams

Fig. 9. Determinant's graph of the system (20) matrix

Fig. 10. Natural shapes of the beam resting on the surface of a half-space with inertial properties

Fig. 11. Natural shapes of the beam resting on the surface of a half-space with distributive properties

Fig. 12. Vertical displacements variability of the entire beam due to the dynamic external load P_5 at each moment

Fig. 13. Vertical displacement variability (y-axis) of the beam at the point, where the dynamic, external load P_5 is applied, with respect to frequency's variation (x-axis)

Fig. 14. Comparison of vertical displacement variability of a beam at the point where the dynamic external load is applied during its action; (I) half-space with inertial properties; (II) half-space with distributive properties

Appendix

1. Background of the applied method:

When studying the fluctuation of a beam with length l and width b resting on the surface of elastic ground, the beam is subjected to the inertia forces oscillating in the mass, the reaction forces in the contact zone, and the external load. The calculation procedure by Zhemochkin and Sinitsyn [15] divides the beam into rectangular elements of equal size c_i (length) and b_i (width) and places in the centre of each element an absolutely rigid liaison to ensure the contact of the beam with the elastic ground surface. Using the mixed method of structural mechanics, the inertia forces oscillating masses are applied only to the beam, while reactions are considered on the beam and on the surface of ground (fig. 1).

Relevant coefficients depend on the beam's deflection and the displacement of the surface of ground. These deflections are determined by the Maxwell-Mohr formula (multiplication of the moment diagrams), and these displacements depend on the model characteristics of the ground. Under the concentrated force applied to a surface of the elastic ground, the displacement of the surface equals infinity. Therefore, the rigid application of forces to the elastic ground surface is considered to be uniformly distributed across the area bc. Free members in the canonical equations system, according to this method, will depend only on the beam's deflections due to (i) the external load and (ii) the inertia's forces of the oscillating masses. Consequently, for free vibration the response of these free members depends only on the inertial forces applied to the beam. The affiliated deflections are defined by using the Maxwell-Mohr formula. The canonical equations permitting determination of the unknowns according to this method take the form of eq. (1):

$$\begin{cases} \sum_{j}^{M} (v_{ij} + y_{ij}) X_j(t) - \sum_{j} y_{ij} J_j(t) + \lambda_i \varphi_0(t) + u_0(t) + \Delta_{iP} = 0; \quad i = 1,K\ ,n \\ \sum_{j}^{M} [X_j(t) - J_j(t)] \lambda_j = I_y \ddot{\varphi}_0(t) \\ \sum_{j} [X_j(t) - J_j(t)] = m \ddot{u}_0(t) \end{cases} \tag{1}$$

Where, $J(t)$ is inertia forces; v is the Green's function defining the displacement of the surface of ground due to the force applied on the same surface and distributed into the elementary area bc; y is the deflection of the beam due to the force applied on the beam; Δ is the function characterizing the system free members; λ is the arm of the elementary masse corresponding to the embedded point; m is the total mass of the beam; and I_y is the inertia moment of the beam corresponding to the axis oy. The unknowns of the system are the liaison efforts $X(t)$, as well as an initial vertical displacement $u_0(t)$, and the angle of rotation $\varphi_0(t)$ of the beam at the embedment point.

2. Transformation of Green's function of the half space surface with inertial properties:

The integrals I_{21} and I_3 after complex transformations issued from the Lamb's problem take the following forms 16]:

$$I_{21} = \int_{1/2}^{1} \Phi_2(\theta) J_0(k\theta r) d\theta . \tag{2}$$

$$I_3 = \int_{1}^{\infty} \Phi_4(\theta) J_0(k\theta r) d\theta \tag{3}$$

where

$$\Phi_2(\theta) = \frac{\theta(1-2\theta^2)^2\sqrt{\theta^2-0.25}}{4\theta^4(\theta^2-1) - \left[1-8\theta^2(1-3\theta^2+2\theta^4)\right]}, \quad \Phi_4(\theta) = \frac{\theta\sqrt{\theta^2-0.25}}{(1-2\theta^2)^2 - 4\theta^2\sqrt{\theta^2-0.25}\sqrt{\theta^2-1}}.$$

The resolutions of these integrals given in 16] are as follow:

$$I_{21}=\sum_{m=1}^{11}\frac{b_{2m-1}}{2m}\left(\,{}_1F_2\left(m;1,m+1;\frac{-k^2r^2}{4}\right)-\frac{{}_1F_2\left(m;1,m+1;\frac{-k^2r^2}{16}\right)}{4^m}\right);\tag{4}$$

$$\begin{aligned}I_3=&\,d_0\left\{\frac{1}{\sqrt{k^2r^2}}-{}_1F_2\left(\frac{1}{2};1,\frac{3}{2};\frac{-k^2r^2}{4}\right)\right\}+\\&+d_1\left\{\frac{\pi}{2}\left[Y_0(\chi kr)+H_0(\chi kr)\right]-\right.\\&\left.-\sum_{m=0}^{\infty}\frac{{}_1F_2\left(\frac{1+m}{2};1,\frac{3+m}{2};\frac{-k^2r^2}{4}\right)}{(1+m)\chi^{m+1}}\right\}+\\&+d_2\left\{\frac{1}{128}\left[-k^4r^4\,{}_2F_3\left(1,1;2,3,3;\frac{-k^2r^2}{4}\right)+\right.\right.\\&\left.\left.+16\left(4-k^2r^2(2-2\gamma+\ln 4)+k^2r^2\ln\left(k^2r^2\right)\right)\right]\right\}\end{aligned}\tag{5}$$

where, d_0, d_1, d_2, b_1, b_3,..., b_{21} are coefficients determined by the least square method. According to Gradshteyn and Ryzhik [20], $H_0(\alpha)$ is the Struve function; $Y_0(\alpha)$ is the Bessel function of the second kind; ${}_pF_q(a;b;d)$ is a generalized hypergeometric function; and $\gamma\approx 0.577216$ the Euler's constant; and $\chi=1.07236$ for $\nu=1/3$.

3. Deflections values of the beam divided into 10 elements:

The deflections values of the beam dividing into 10 identical elements with length c, obtained using the multiplication of the moment's diagrams method are as follows:

$$\frac{c^3}{EI}\begin{bmatrix}
y_{11}=\frac{243}{8} & y_{12}=\frac{245}{12} & y_{13}=\frac{275}{24} & y_{14}=\frac{9}{2} & y_{15}=\frac{13}{24} & y_{16}=0 & y_{17}=0 & y_{18}=0 & y_{19}=0 & y_{110}=0 \\
 & y_{22}=\frac{343}{24} & y_{23}=\frac{25}{3} & y_{24}=\frac{27}{8} & y_{25}=\frac{5}{12} & y_{26}=0 & y_{27}=0 & y_{28}=0 & y_{29}=0 & y_{210}=0 \\
 & & y_{33}=\frac{125}{24} & y_{34}=\frac{9}{4} & y_{35}=\frac{7}{24} & y_{36}=0 & y_{37}=0 & y_{38}=0 & y_{39}=0 & y_{310}=0 \\
 & & & y_{44}=\frac{9}{8} & y_{45}=\frac{1}{6} & y_{46}=0 & y_{47}=0 & y_{48}=0 & y_{49}=0 & y_{410}=0 \\
 & & & & y_{55}=\frac{1}{24} & y_{56}=0 & y_{57}=0 & y_{58}=0 & y_{59}=0 & y_{510}=0 \\
 & & & & & y_{66}=y_{55} & y_{67}=y_{45} & y_{68}=y_{35} & y_{69}=y_{25} & y_{610}=y_{15} \\
 & \textit{Sym} & & & & & y_{77}=y_{44} & y_{78}=y_{34} & y_{79}=y_{24} & y_{710}=y_{14} \\
 & & & & & & & y_{88}=y_{33} & y_{89}=y_{23} & y_{810}=y_{13} \\
 & & & & & & & & y_{99}=y_{22} & y_{910}=y_{12} \\
 & & & & & & & & & y_{1010}=y_{11}
\end{bmatrix}$$

Appendix's legends figures

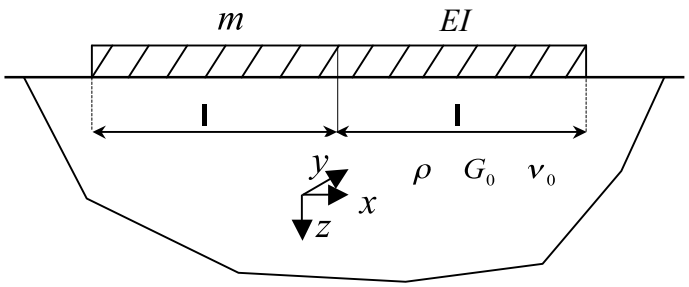

Fig.1.

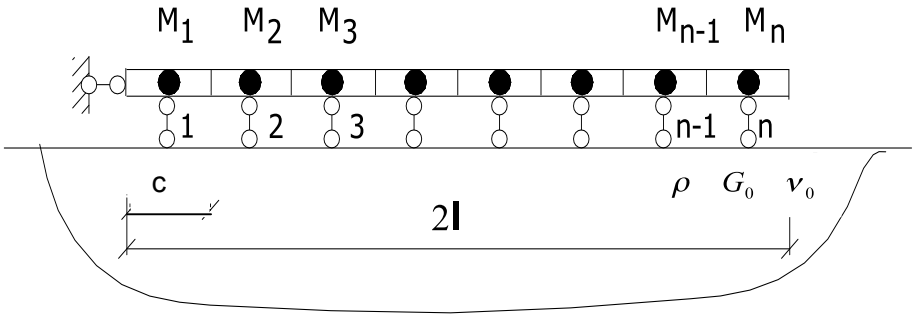

Fig.2.

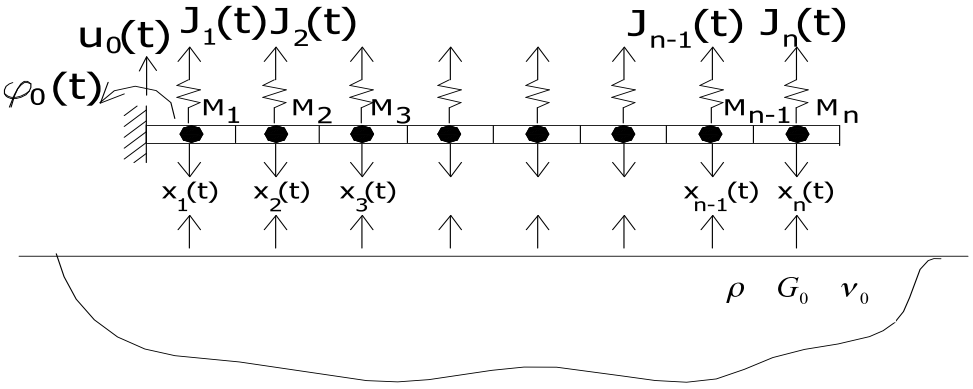

Fig.3.

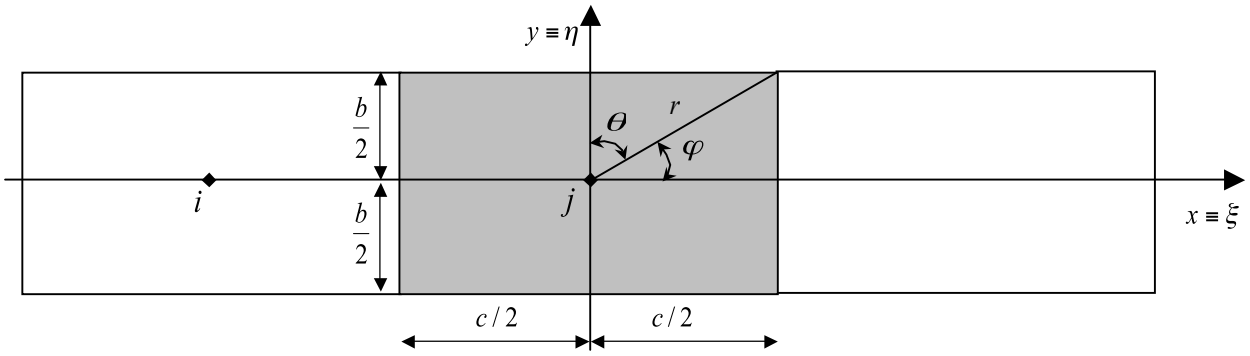

Fig.4.

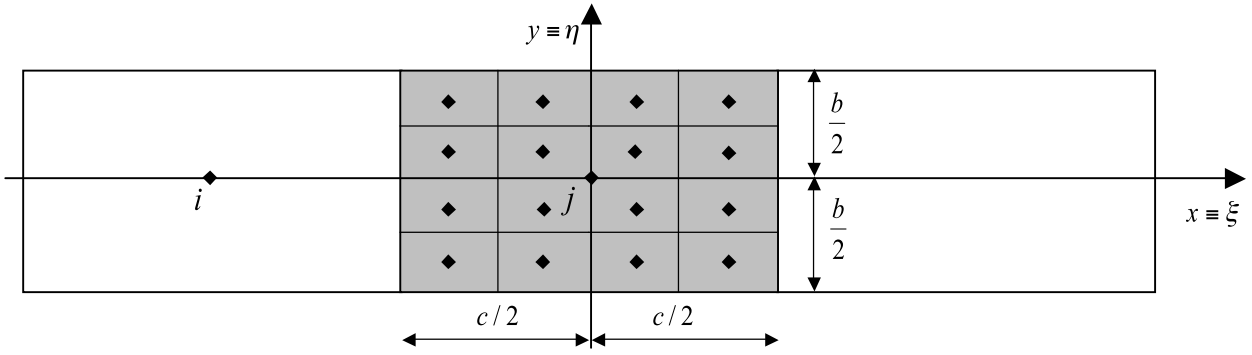

Fig.5.

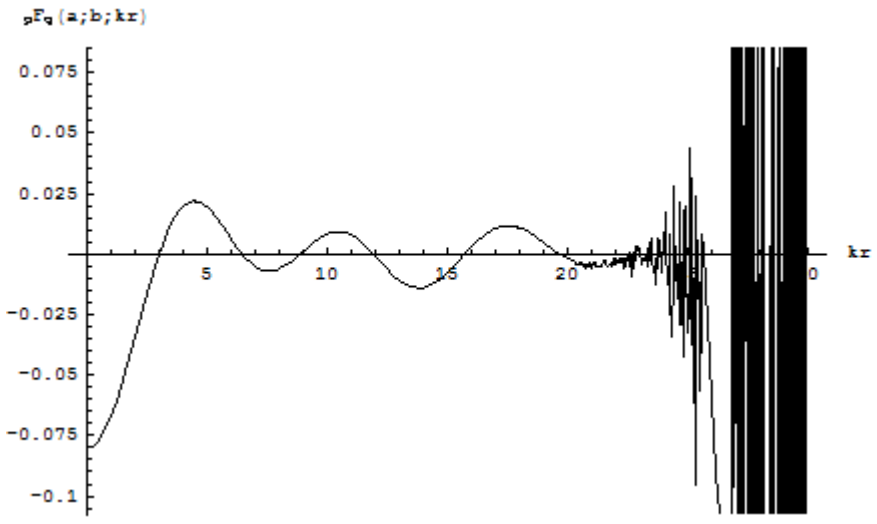

Fig.6.

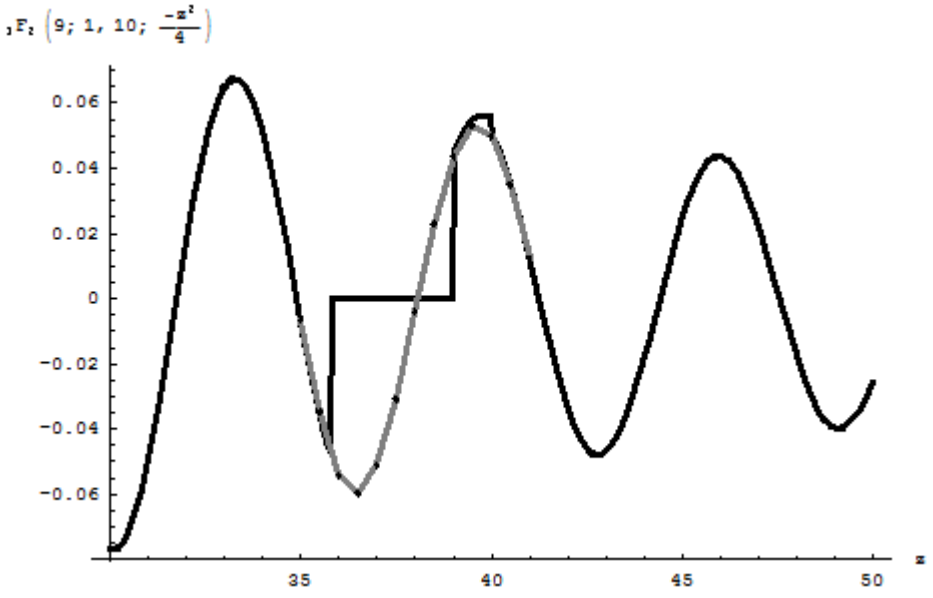

Fig.7.

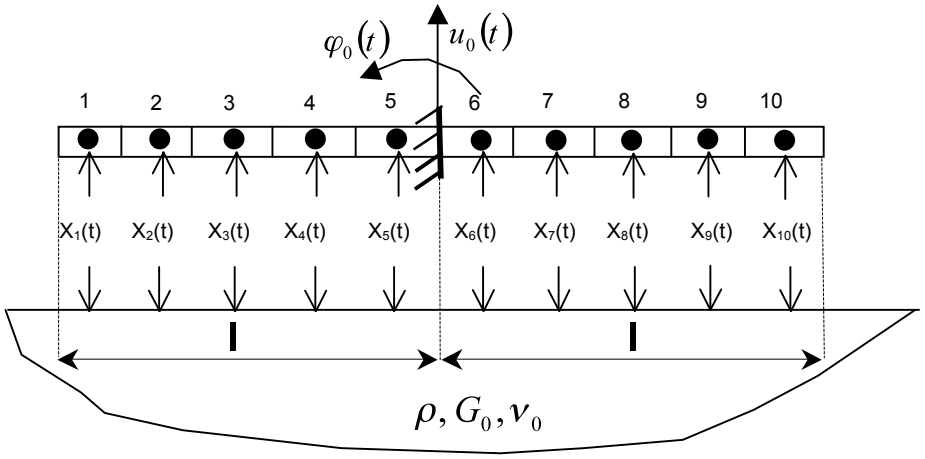

Fig.8.

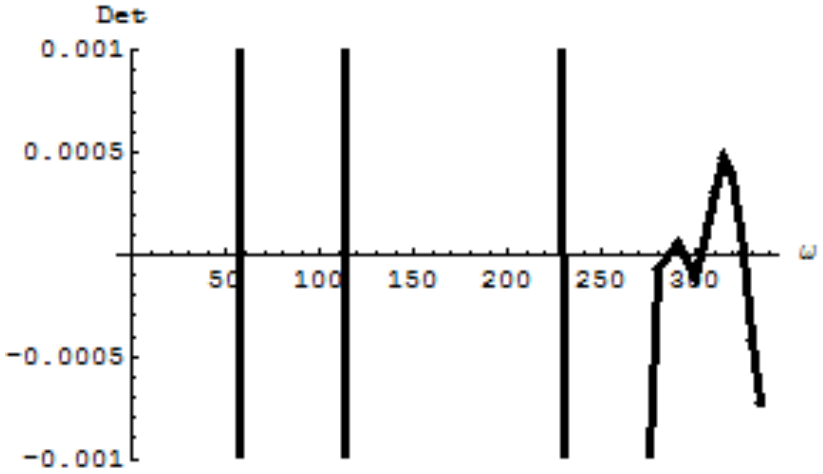

Fig.9.

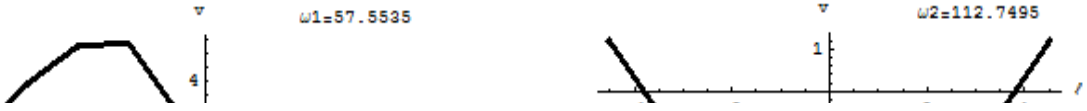

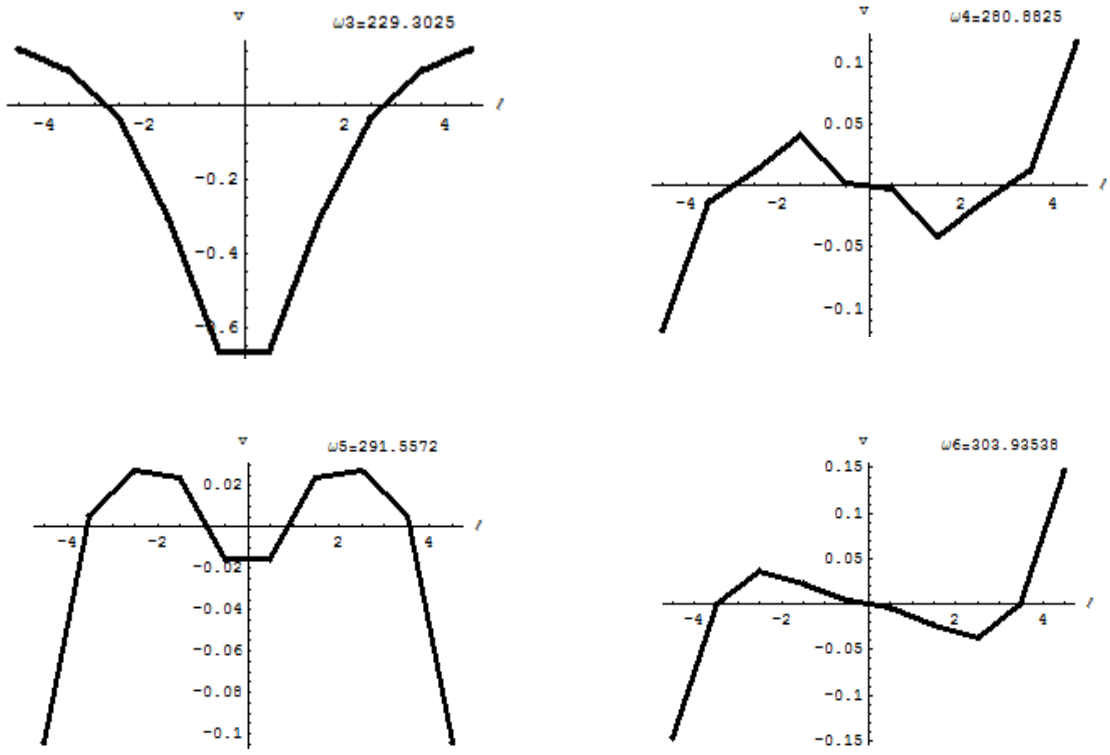
ω3=229.3025
ω4=280.8825
ω5=291.5572
ω6=303.93538

Fig.10.

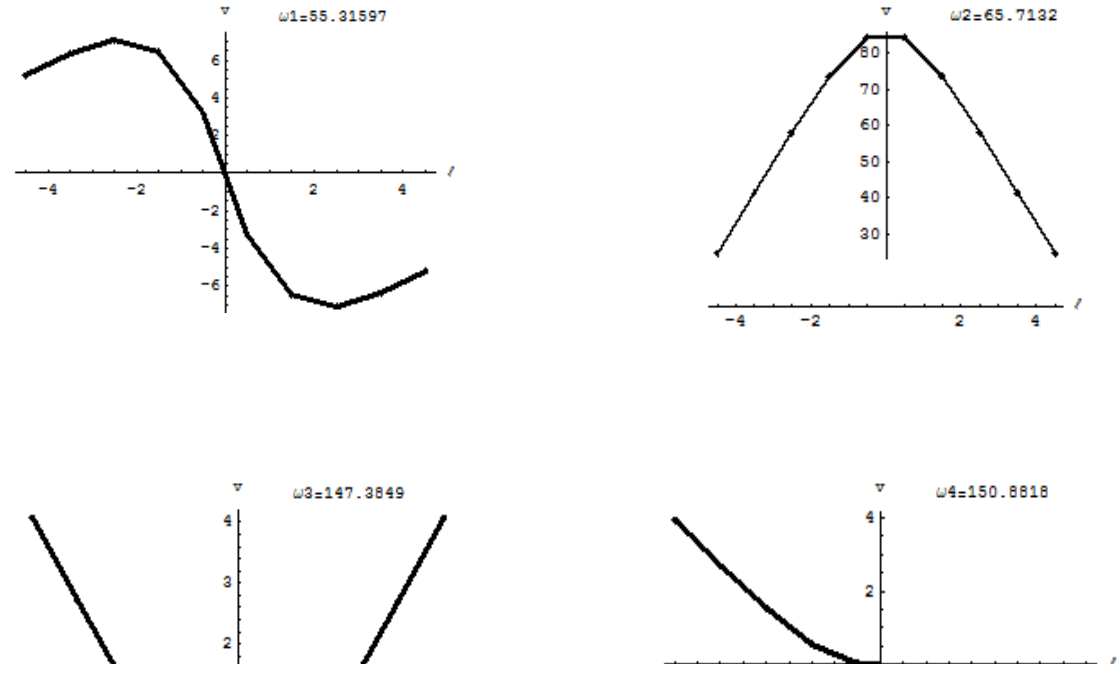
ω1=55.31597
ω2=65.7132
ω3=147.3849
ω4=150.8818

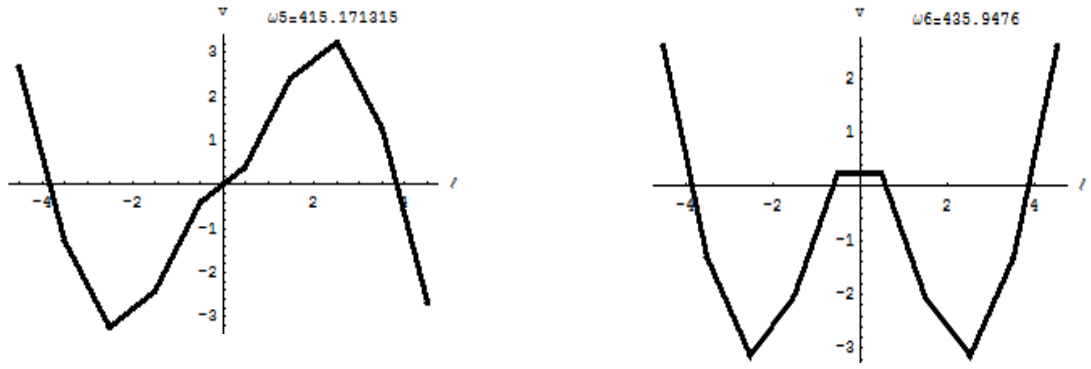
v
ω5=415.171315
l
v
ω6=435.9476
l

Fig.11.

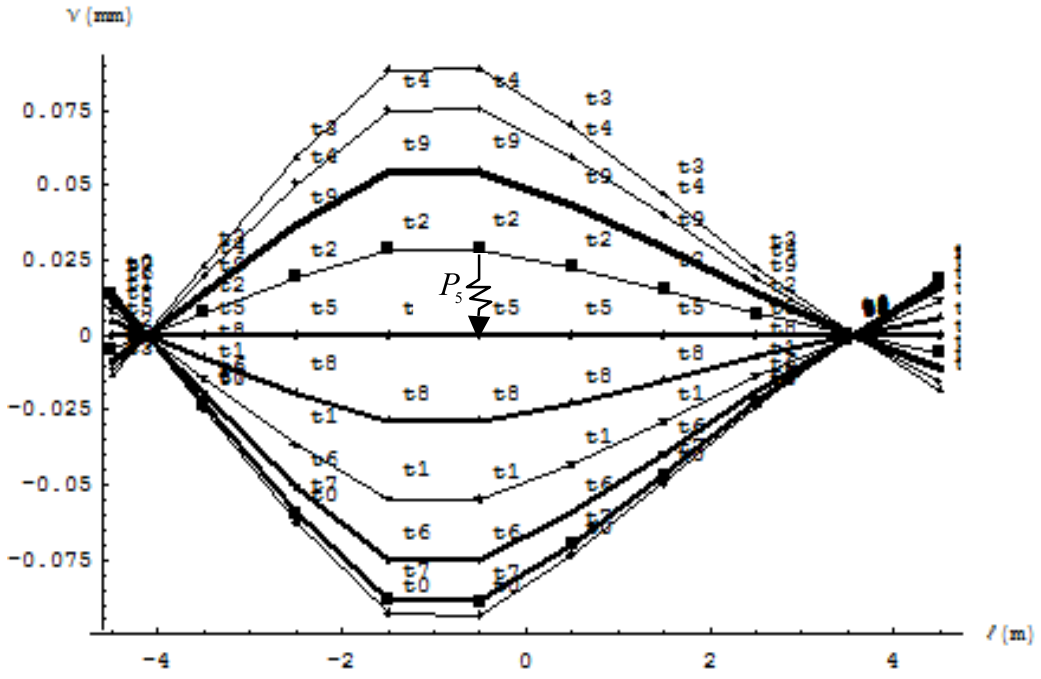
v (mm)
0.075
0.05
0.025
0
-0.025
-0.05
-0.075
P_5
l (m)
-4
-2
0
2
4

Fig.12.

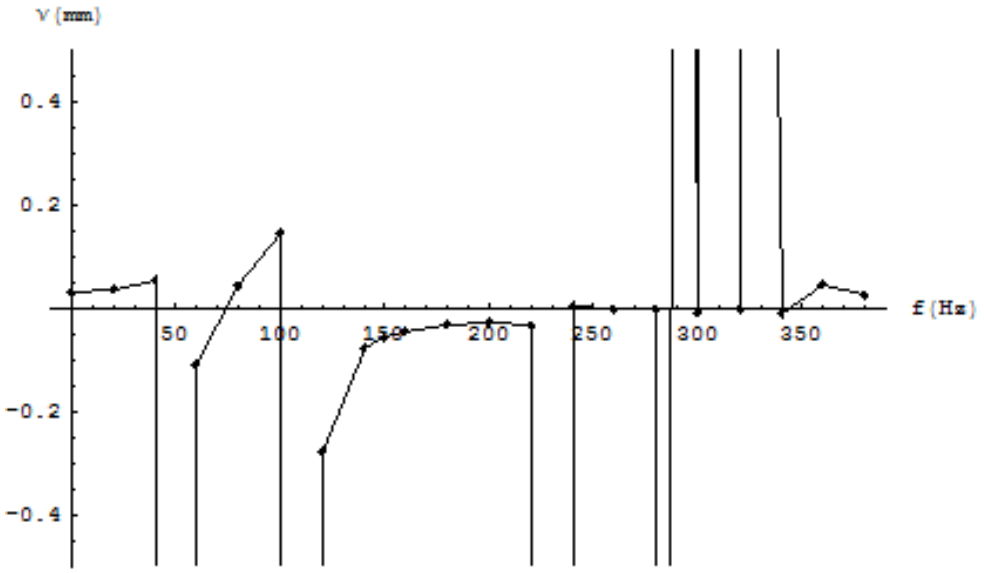
V (mm)
0.4
0.2
-0.2
-0.4
50
100
150
200
250
300
350
f (Hz)

Fig.13.

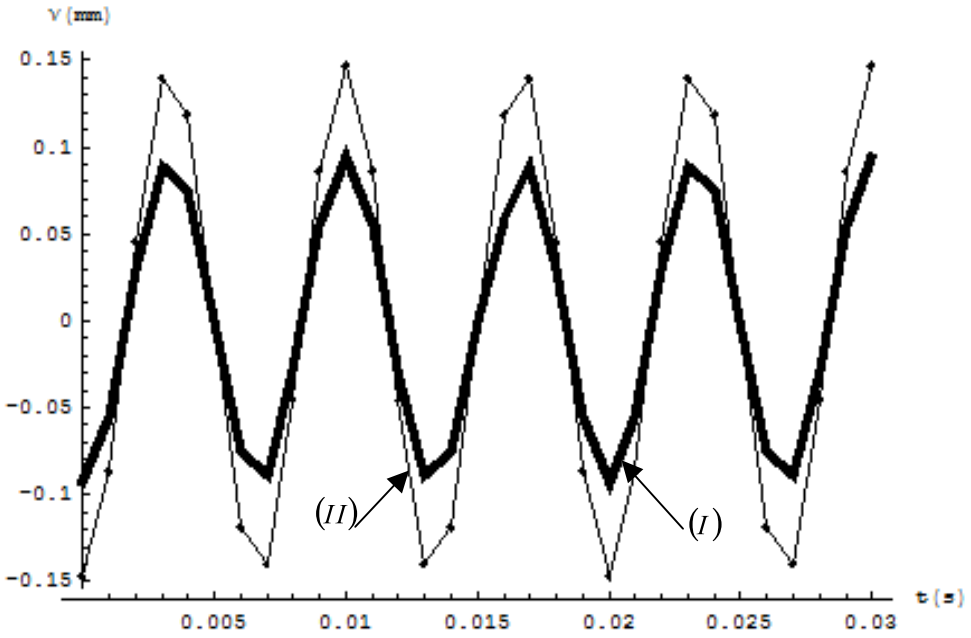
V (mm)
0.15
0.1
0.05
0
-0.05
-0.1
-0.15
0.005
0.01
0.015
0.02
0.025
0.03
t (s)
(II)
(I)

Fig.14.

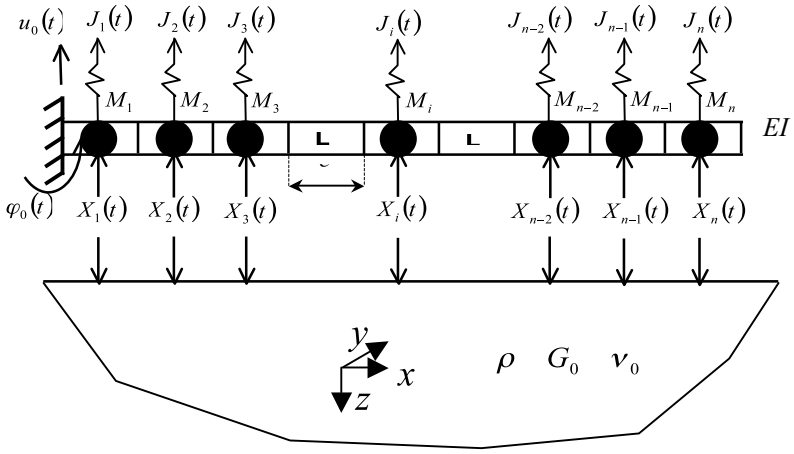

Appendix Fig.1.